Antiferromagnetism in high temperature superconductors

Efstratios Manousakis
Department of Physics and Center for Materials Research and Technology, Florida State University, Tallahassee, Florida 32306

Abstract

We offer a brief overview of the main common features of the antiferromagnetism in the copper-oxide based high temperature superconductors. We also discuss the nature of the carriers created upon light doping such quantum antiferromagnets.

I. INTRODUCTION

The crystal structure of all copper-oxide superconductors contains CuO_2 planes. The electric charge of these planes in the materials is determined by the other elements contained in the structure. Independently of the nature of the background elements when the charge of these planes is $+2e$ per CuO_2 unit cell, the material behaves as an almost ideal two-dimensional spin-1/2 quantum antiferromagnet with very weak coupling between successive copper-oxide planes [1]. In the above charge configuration the material is a Mott insulator, and when its charge deviates from this value, say to $+(2+x)e$, then we shall call this material a doped antiferromagnet where, for positive (negative) x we have created a fraction of x carriers in the form of holes (electrons).

Our understanding of the antiferromagnetism of the parent compounds of the copper oxide superconductors is heavily based on the properties of the pure two-dimensional spin-1/2 isotropic quantum Heisenberg antiferromagnet:

$$H = J \sum_{<ij>} \vec{s}_i \cdot \vec{s}_j \tag{1}$$

where the sum is over all planar nearest neighbors and $\vec{s}_i$ are the spin-1/2 operators. The only parameter of the model, the antiferromagnetic coupling J, can be found by using one set of experimental data. We shall see that only one parameter is enough to understand quantitatively the nature of the magnetic excitations revealed by the neutron and the Raman scattering experiments from the undoped insulators, such as La_2CuO_4. In this paper, we shall review these experiments and compare them to the theory. In addition, the roles of small anisotropies and of the weak interplanar coupling in the real materials will be discussed.

The fundamental question which arises next is what happens when one introduces a small amount of carriers inside such an almost ideal quantum antiferromagnet. We shall study the motion of a single hole inside a quantum antiferromagnet by means of a self-consistent perturbation approach. We have shown that this approach is accurate by comparing our results on small size lattices to those obtained by exact diagonalization. The calculated single hole spectrum shares several features with the

results of angle resolved photoemission experiments. For example, they agree in the bandwidth and in the location of the band minimum at a non-trivial position of the Brillouin zone (at $(\pi/2, \pi/2)$). These two features are very different from those found in standard band structure calculations. There are, however, regions of the Brillouin zone around $(\pi, 0)$ where the calculations and experiments disagree. We shall also discuss that the disagreement between theory and experiment around $(\pi, 0)$ can be accounted for by including a hole-hopping term which allows the hole to directly hop along a diagonal of the square lattice of the copper-oxide plane. In addition, the resolution in these experiments is insufficient to verify additional interesting features of the nature of the charged quasiparticle created by the introduction of the hole in a quantum antiferromagnet as found by our method. Such features are additional excited states of the quasiparticle which we call string states; these states exist because the mobile hole locally sees an almost linear potential.

II. THE UNDOPED INSULATOR

A. Antiferromagnetic order at half-filling

The transition to an antiferromagnetic state in La_2CuO_4 was first observed in a powder diffraction study [2] where it was found that the staggered moment at $T = 0$ is about $0.5 \pm 0.1\mu_B$. The existence of the long range order was independently confirmed by muon-spin rotation experiments [3]. From the integrated intensity of the antiferromagnetic Bragg peak [4,5] one finds that the zero-temperature staggered magnetization is strongly sample dependent and is correlated to the oxygen content of the sample. For the crystal with the highest $T_N \sim 300K$, Yamada et al. [4] find $m^\dagger \sim 0.6\mu_B$ which is close to the value found by several calculations using the isotropic spin-$\frac{1}{2}$ antiferromagnetic Heisenberg model (AFHM) on the square lattice [1].

B. Spin correlations

In neutron scattering experiments the correlation length is extracted from the static structure factor $S(q)$ which is obtained by integrating the measured spin-dynamic structure function up to the energy of the incident neutron. Endoh et al. [5] have approximated the structure function by $S(q) \sim 1/(q^2 + (1/\xi(T))^2)$ and used this expression to extract an estimate of the $2D$ correlation length. In Fig. 1, we plot the inverse correlation length versus T as observed by neutron scattering experiments. The solid curve is obtained using the expression

$$\xi(T) = C_\xi exp(2\pi\rho_s/T) \tag{2}$$

which fits the theoretical results obtained from the spin-$\frac{1}{2}$ AFHM on the square lattice (or the equivalent nonlinear σ model). The most accurate results are $\rho_s = 0.20J$ and $C_\xi = 0.276a_H$ obtained as in Ref. [1]. In the plots we use $a_H = 3.8\mathring{A}$ as the $Cu - Cu$ distance. The solid line is obtained from the theoretical expression with $J = 1480K$. The data disagree with the theoretical curves for correlation lengths on the order of $200\mathring{A}$ or larger. These differences and the fact that crystals with higher T_N give

somewhat different correlation lengths can be attributed to the high sensitivity of the spin-correlation length to the hole concentration x [1].

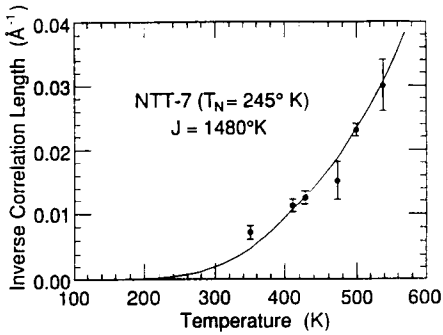

Fig. 1: Comparison between measured and calculated inverse correlation length as a function of temperature.

C. Spin-wave excitations

Aeppli et al. [6], using high-energy inelastic neutron scattering and constant energy transfer ω scans, measured the intensity of the outgoing neutrons as a function of the momentum transfer q (see Fig. 2).

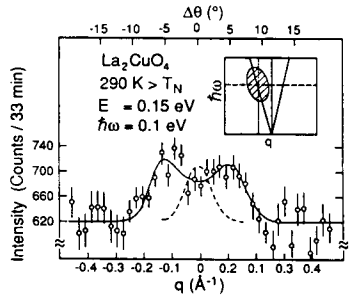

Fig. 2: Neutron scattering intensity. Constant-energy transfer scan, collected in the transverse direction for momentum transfers near (2,0,1).

The solid-line fit shows two peaks which correspond to two spin-wave excitations, one traveling with $\vec{q}$ and the other with $-\vec{q}$. This fit gives a spin-wave velocity of $\hbar c = 0.78eV - \mathring{A}$. Repeating the experiment at different energy transfers, Aeppli et al. find that their data can be explained in the long-wavelength limit by the spin-wave expression $\omega_q = cq$ with $\hbar c = 0.85 \pm 0.03eV - \mathring{A}$. Theoretical studies of the spin-1/2 AFHM on the square lattice give $c = Z_c\sqrt{2}Ja$ with values for Z_c lying around $Z_c \simeq 1.19 \pm 0.05$. Using this value for Z_c and $c = 0.85eV - \mathring{A}$ inferred form these neutron scattering studies, we obtain $J \simeq 1540 \pm 60K$ in excellent agreement with that obtained by comparing the correlation lengths.

Raman scattering studies [7] of La_2CuO_4 have revealed a high frequency peak which has been attributed to scattering from magnon pairs with opposite momenta. The Hamiltonian describing the scattering of light of incident polarization $\mathbf{E_1}$ into a

scattered light of polarization $\mathbf{E_2}$ by a magnon pair is given as

$$H_R = A \sum_{<ij>} (\mathbf{E_1} \cdot \hat{e}_{ij})(\mathbf{E_2} \cdot \hat{e}_{ij})(\vec{s}_i \cdot \vec{s}_j), \tag{3}$$

where $\hat{e}_{ij}$ the unit vector connecting n.n. sites. The scattering intensity $I(\omega)$ depends strongly on the light polarization relative to the crystallographic axes. The strong 2D dimensional nature of the magnetism in La_2CuO_4 is evidenced by the strong dependence of the peak on the polarization direction of the incident and scattered waves. For example, there is no peak when $\mathbf{E_1}||\hat{z}$ and $\mathbf{E_2}||\hat{z}$, with z being the direction perpendicular to the copper-oxygen plane.

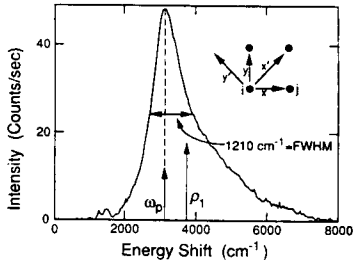

Fig. 3: The Raman scattering intensity obtained by Lyons et al.

In Fig. 3 we show the data obtained by Lyons et al. [7] for $\mathbf{E_1}||\hat{x}'$ and $\mathbf{E_2}||\hat{y}'$ where the directions $\hat{x}$ and $\hat{y}$ are the unit vectors connecting copper atoms on the CuO_2 plane and $\hat{x}'$ and $\hat{y}'$ are along the diagonal of the square lattice formed by the copper atoms (see inset of Fig. 3). An estimate for J can be obtained from the moments ρ_n of the Raman scattering intensity. These moments have been calculated by a high temperature series expansion [8], exact diagonalization [9] on small size lattices and by a variational Monte Carlo calculation [10] on large size lattices. These studies give good agreement with the values of the moments obtained by integrating the Raman scattering intensity with the same value of $J \sim 1500K$.

D. Metamagnetism

The interplanar coupling J' is of the order of $10^{-5}J$ and has a small effect on the two-dimensional (2D) spin-correlations above the 3D Nèel ordering temperature. Furthermore, the zero temperature properties calculated for an isolated CuO_2 plane are only weakly affected by such a small value of J'. The role of possible Ising-like anisotropies have been examined by considering different values for couplings J_x, J_y, J_z, i.e.,

$$H = \sum_{<ij>} (J_x S_i^x S_j^x + J_y S_i^y S_j^y + J_z S_i^z S_j^z) \tag{4}$$

and have been found to be weak. It has been found, however, that the antisymmetric term

$$H_a = J^{bc} \sum_{<ij>} (\vec{S}_i \times \vec{S}_j) \cdot \hat{a}, \tag{5}$$

is needed to explain a hidden ferromagnetic behavior manifesting itself below T_N. This term is responsible for the canting of the spins away from the direction of the staggered magnetization (which lies in the $\hat{a}$-$\hat{c}$ plane) along the direction towards the $\hat{b}$ axis by a small angle. This term arises from the rotation of the CuO_6 octahedra around the Cu site in the unit cell. Using such antisymmetric term, Thio et al. have qualitatively explained the behavior of the uniform susceptibility and their magnetoresistance data. Later neutron scattering [12] provided direct evidence for the canting of the spins out of the CuO_2 planes. The coupling J^{bc}, estimated from the angle of the canted spins, was found to be small compared to the antiferromagnetic coupling J ($J^{bc}/J \sim 10^{-3}$) and can be neglected in the calculation of the 2D correlation length and staggered magnetization.

III. THE NATURE OF THE CHARGE CARRIER

The question that arises next, namely what happens if we introduce charge carriers inside such a quantum Heisenberg antiferromagnet, is still open. The approach described below has been seriously pursued by the theoretical community over the past five years. The motion of a single-hole in an antiferromagnetically aligned spin background is a longstanding problem [13] concerning the electron states in localized magnetic insulators and has been studied considerably. A single-hole is not in a simple Bloch state since by hopping it disturbs the antiferromagnetic arrangement of spins and thus destroys the translational invariance. One of the simplest models for studying this problem is the $t-J$ model given as

$$\hat{H}_{t-J} = -t \sum_{<i,j>\sigma} (\bar{c}^{\dagger}_{i,\sigma}\bar{c}_{j,\sigma} + H.c.) + J \sum_{<i,j>} \vec{S}_i \cdot \vec{S}_j, \tag{6}$$

where $\bar{c}_{i,\sigma}$ is the constrained hole creation operator defined as $\bar{c}_{i,\sigma} = c_{i,\sigma}(1 - c^{\dagger}_{i,-\sigma}c_{i,-\sigma})$, while $c_{i,\sigma}$ denotes the annihilation operator for an electron with spin σ on the lattice site i and the hole number operator is denoted by $\hat{n}^h_i$. This model is a simple extension of the spin-1/2 AFHM to include hole hopping. This Hamiltonian operates inside a subspace of the Hilbert space containing only singly occupied states. The doubly occupied states have been integrated out, and their effect is to give rise to the Heisenberg exchange term.

A. Motion of a single hole

There is no method to treat the Hamiltonian (6) exactly. We followed a self-consistent perturbation approach, and we have shown that it works accurately for $t >> J$. Our method can be used to obtain the single hole spectral function on large size lattices. On small size lattices it is possible to diagonalize the $t-J$ Hamiltonian, and thus we are able to compare our results with the exact solutions. The agreement is very good, which allows us to believe our results on much larger size lattices.

We make the assumptions that the spin part of the $t-J$ Hamiltonian has an antiferromagnetically long-range ordered ground state and that the excitations are spin waves. Since the spin-wave approximation works accurately for the spin part of the $t-J$ model it is natural to extend this treatment to the case of a single hole.

Let us define the hole operators such that $h_i = c^\dagger_{i\uparrow}$ on the $\uparrow$ sublattice and $f_i = c^\dagger_{i\downarrow}$ on the $\downarrow$ sublattice. The other hole operators can be written as

$$c_{i\downarrow} = h^\dagger_i a_i, \quad a_i = S^\dagger_i \quad i \in \uparrow; \qquad c_{i\uparrow} = f^\dagger_i b_i, \quad b_i = S^-_i \quad i \in \downarrow . \tag{7}$$

In the linear spin-wave approximation one keeps terms only up to quadratic in the hard-core boson operators in both the Heisenberg and hopping terms of Eq. (6) and diagonalizes the J term using the standard approach of spin-wave theory for antiferromagnets, namely by means of a Bogoliubov transformation. In this approximation the hopping term couples the holes with the spin-waves as

$$\hat{H}t = \sum_{\vec{k},\vec{q}} g(\vec{k},\vec{q})\Big\{h^\dagger_{\vec{k}} f_{\vec{k}-\vec{q}}\alpha_{\vec{q}} + f^\dagger_{\vec{k}} h_{\vec{k}-\vec{q}}\beta_{\vec{q}}\Big\} + H.c., \tag{8}$$

where

$$g(\vec{k},\vec{q}) = tz\sqrt{\frac{2}{N}}(u_q\gamma_{\vec{k}-\vec{q}} + v_q\gamma_{\vec{k}}). \tag{9}$$

$$u_{\vec{k}} = [(1-\gamma^2_{\vec{k}})^{-1/2} + 1]^{1/2}/\sqrt{2}, \tag{10}$$

$$v_{\vec{k}} = -sgn(\gamma_{\vec{k}})[(1-\gamma^2_{\vec{k}})^{-1/2} - 1]^{1/2}/\sqrt{2}, \tag{11}$$

and $\gamma_{\vec{k}} = \sum_{\vec{\delta}} e^{i\vec{k}\cdot\vec{\delta}}/z$, and z is the number of the nearest-neighbors. The α's and β's are spin-wave operators related to the a's and b's via the Bogoliubov transformation $\alpha_{\vec{q}} = u_q a_{\vec{q}} - v_q b^\dagger_{-\vec{q}}$ and $\beta_{\vec{q}} = u_q b_{-\vec{q}} - v_q a^\dagger_{\vec{q}}$ and they both follow the dispersion $\Omega_{\vec{q}} = JzS\sqrt{1-\gamma^2_{\vec{q}}}$. The J part of the Hamiltonian takes the diagonal form $H_J = \sum_{\vec{q}} \Omega_{\vec{q}}(\alpha^\dagger_{\vec{q}}\alpha_{\vec{q}} + \beta^\dagger_{\vec{q}}\beta_{\vec{q}})$.

In the limit $J << t$, using a self-consistent perturbation approach where only non-crossing diagrams are summed, one obtains [15,14,16] the following expression for the hole propagator

$$G(\vec{k},\omega) = \frac{1}{\omega - \sum_{\vec{q}} g^2(\vec{k},\vec{q})G(\vec{k}-\vec{q},\omega-\Omega_{\vec{q}})}. \tag{12}$$

We give the numerical solutions obtained by iterating Eq. (12) on finite clusters of size $N = L \times L$.

B. The String Picture

In Fig. 4 we give the calculated spectral function $A(\vec{k},\omega) = 1/\pi ImG(\vec{k},\omega)$ as a function of ω for several values of $\vec{k}$. In Fig. 5 we give the function $E(\vec{k})$, namely the lowest energy peak for given value of $\vec{k}$ along the path of the Brillouin zone shown in the inset. Notice that the minimum of the band is at $\vec{k} = (\pi/2, \pi/2)$. The spectral function for this value of $\vec{k}$ has a well defined low energy peak. In addition, however, it has a series of higher energy peaks of decreasing strength with increasing energy of the peak. These series of higher energy peaks in the spectral function have been analyzed in Ref. [16] and they can be understood as follows. In the limit $t >> J$

the hole moves faster than the time required for the spins in the neighborhood of the hole to relax; because the spins are in an antiferromagnetically ordered state, the hole "sees" an almost linearly rising potential as a function of the distance from the "birth" place of the hole. This can become clear if one considers instead of the $t-J$ model the $t-J_z$ model where quantum spin fluctuations are eliminated. In this case it can be shown that there is a linear potential which traps the hole around its birth place and it gives rise to a series of well defined levels separated by an energy difference that scales as $(J/t)^{2/3}$. The presence of quantum spin fluctuations does not alter the qualitative picture but gives rise to a finite width to these states.

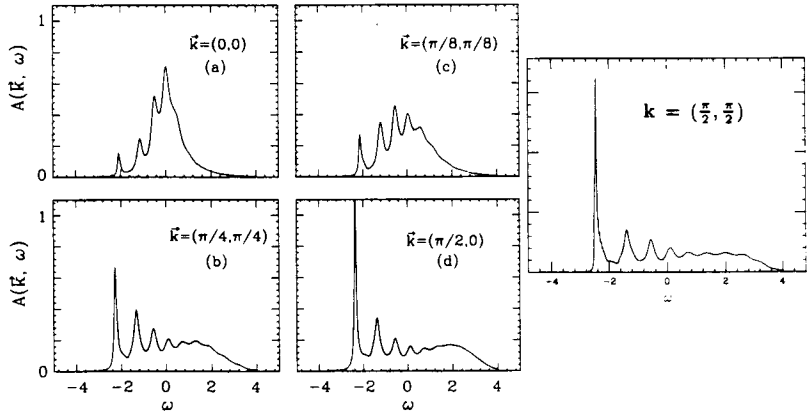

Fig. 4: The hole spectral function for several values of $\vec{k}$.

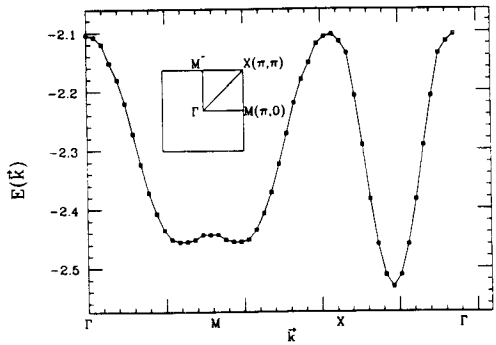

Fig. 5: The energy $E(\vec{k})$ of the lowest energy peak for different $\vec{k}$.

C. Photoemission Experiments

Very recently [17] a high resolution angle resolved photoemission experiment has been performed on the insulating layered copper-oxide $Sr_2CuO_2Cl_2$. The energy dispersion $E(\vec{k})$ along the same path of the Brillouin zone as that shown in the inset

of Fig. 5 is plotted in Fig. 6. The authors of Ref. [17] compare their experimental results with the theoretical prediction [16] shown as the solid line in Fig. 6.

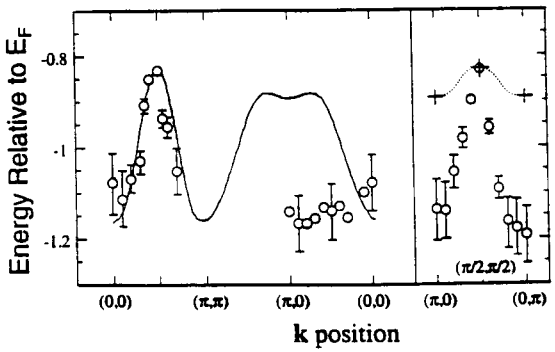

Fig. 6: The results of the angle resolved photoemission measurements [17] on the insulating $Sr_2Cu_2O_2Cl_2$ is compared with the theoretical $E(\vec{k})$.

The experimental value of the bandwidth $W = 280 \pm 60meV$ is an order of magnitude smaller than the bandwidth calculated by standard band structure calculations [18] (these calculations give $W \sim 3eV$). As we have already discussed [1] the value of the Heisenberg antiferromagnetic coupling has been determined to be approximately $J = 125meV$. The value of W for this value of $J/t \simeq 0.3$ obtained in our $t-J$ model calculation is approximately $W = 2.2J$, which is in excellent agreement with the experimental value. The additional feature that agrees with the experiment is the location of the peak, at $k = (\pi/2, \pi/2)$, which is a non-trivial prediction of the $t-J$ model.

There is a disagreement between theory and experiment at values of $\vec{k} = (\pi, 0)$ as can be noticed in Fig. 6. We believe that this disagreement can be partially removed by adding a t' term in the $t-J$ model Hamiltonian namely a term that allows the hole to hop along the diagonal of the square lattice. We performed a self consistent calculation in the spirit of Ref. [16] and we found that by taking $t' \simeq 70meV$ as found in Ref. [19], the overall bandwidth is reduced by a small amount but around $\vec{k} = (\pi, 0)$, $E(\vec{k})$ is significantly lowered relative to the value at $\vec{k} = (\pi/2, \pi/2)$.

In addition, it is clear that the resolution in the photoemission experiments is insufficient to resolve the multiple peak structure which supports the "string" picture discussed earlier.

IV. ACKNOWLEDGEMENTS

This work was supported in part by the U. S. Office of Naval Research under grant No. N00014-93-1-0189. I wish to thank C. S. Hellberg for his careful reading of the manuscript and his comments.

REFERENCES

[1] E. Manousakis, Rev. of Mod. Phys. **63**, 1 (1991).

[2] D. Vaknin, S.K.Sinha, D.E. Moncton, D.C. Johnston, J.M. Newsam, C.R. Safinya and H.E. King, Jr., 1987, Phys. Rev. Lett. **58**, 2802.

[3] Y. J. Uemura, W. J. Koessler, X. H. Yu, J. R. Kempton, H. E. Schone, D. Opie, C. E. A. Stronach, D.C. Johnston, M. S. Alvarez and D. P. Goshorn, 1987, Phys. Rev. Lett. **59**, 1045.

[4] K. Yamada, E. Kudo, Y. Endoh, Y. Hidaka, M. Oda, M. Suzuki and T. Murakami, 1987, Solid State Communications, **64**, 753.

[5] Y. Endoh, K. Yamada, R. J. Birgeneau, D.R., Gabbe, H. P. Jenssen, M. A. Kastner, C. J. Peters, P. J. Picone, T. R. Thurston, J. M. Tranquada, G. Shirane, Y. Hidaka, M. Oda, Y. Enomoto, M. Suzuki, and T. Murakami, 1988, Phys. Rev., **B37**, 7443.

[6] G. Aeppli, S. M. Hayden, H. A. Mook, Z. Fisk, S-W. Cheong, D. Rytz, J. P. Remeika, G. P. Espinosa, and A. S. Cooper, 1989, Phys. Rev. Lett. **62**, 2052.

[7] K. B. Lyons, P.A. Fleury, J.P.Remeika, A. S. Cooper, and T.J. Nergan, 1988, Phys. Rev. **B37**, 2353.

[8] R. Singh, P. Fleury, K. Lyons, and P. Sulewski, Phys. Rev. Lett. **62**, 2736 (1989).

[9] E. Dagotto and D. Poilblanc, Phys. Rev. **B 42**, 7940 (1990); E. Gagliano and S. Bacci, *ibid.* **42**, 8772 (1990).

[10] Z. Liu and E. Manousakis, Phys. Rev. **B 43**, 13246 (1991).

[11] T. Thio et al., Phys. Rev. **B 38**, 905 (1988).

[12] M. A. Kastner, et al., 1988, Phys. Rev. **B38**, 6636.

[13] W. F. Brinkman and T. M. Rice, Phys. Rev. B **2**, 1324 (1970).

[14] S. Schmitt-Rink, C. M. Varma, and A. E. Ruckenstein, Phys. Rev. Lett., **60**, 2793 (1988).

[15] C. Kane, P. Lee, and N. Read, Phys. Rev. B **39**, 6880 (1989).

[16] Z. Liu and E. Manousakis, Phys. Rev. B **44**, 2414 (1991); *ibid*, **45**, 2425 (1991).

[17] B. O. Wells, Z. -X. Shen, A. Matsuura, D. M. King, M. A. Kastner, M. Greven and R. J. Birgeneau, MIT, Preprint.

[18] W. E. Pickett, Rev. Mod. Phys. **61**, 433 (1989).

[19] M. S. Hybertsen, E. B. Stechel and D. R. Jennison, Phys. Rev. **B 41**, 11068 (1990).